

BRNO UNIVERSITY OF TECHNOLOGY  
FACULTY OF MECHANICAL ENGINEERING  
INSTITUTE OF AUTOMOTIVE ENGINEERING

**Ing. Adam Vondrák**

**FITTING AND EXTRAPOLATION OF TURBOCHARGER TURBINE MAPS**  
PROKLÁDÁNÍ A EXTRAPOLACE MAP TURBODMYCHADLOVÝCH TURBÍN

Field of study: Construction and Process Engineering  
Edition: Shortened version of Ph.D. thesis  
Supervisor: prof. Ing. Josef Štětina, Ph.D.

**Keywords**

turbine, map, fitting, extrapolation, turbocharger, turbocharging

**Klíčová slova**

turbína, charakteristika, prokládání, extrapolace, turbodmychadlo, přeplňování

The original manuscript is archived in the library of the Faculty of Mechanical Engineering in Brno.

© Adam Vondrák, 2021

ISBN 80-214-

ISSN 1213-4198

# CONTENTS

GOALS OF THE PH.D. THESIS .....	5
INTRODUCTION .....	6
1 TURBOCHARGING .....	7
2 BASELINE TURBINE FITTING METHOD.....	10
2.1 Pre-Processing of Input Data .....	10
2.2 Fitting the Optimum Blade Speed Ratio .....	10
2.3 Fitting the Maximum Efficiency .....	12
2.4 Fitting the Normalized Efficiency.....	13
2.5 Fitting the Optimum Corrected Mass Flow Rate .....	13
2.6 Fitting the Normalized Mass Flow Rate .....	14
2.7 Optimization.....	15
3 NEW TURBINE FITTING ALGORITHM.....	17
3.1 Radial Equilibrium.....	17
3.2 Ideal Nozzle Analogy.....	17
3.3 Optimum Corrected Speed Limitation.....	19
4 VALIDATION OF THE PROPOSED METHODOLOGY .....	21
4.1 Engine Performance Simulation – Steady State .....	22
4.2 Engine Performance Simulation – Transient .....	23
CONCLUSION .....	25
REFERENCES .....	27
AUTHOR’S CV .....	29
ABSTRACT .....	30



## **GOALS OF THE PH.D. THESIS**

The main goals of this Ph.D. thesis are:

- Explain the reasons for the modelling of turbine performance and introduce the context of turbocharged engine working cycle simulations.
- Research a relevant turbine modelling method that is being used in the industry (potentially as part of a commercial software product).
- Develop a custom code for fitting and extrapolation of measured turbine maps and integrate it into an application with a graphical user interface.
- Use optimization methods to minimize the error between the measured data and the turbine performance models.
- Validate the new algorithm and run engine performance simulations to evaluate any potential differences from the results obtained using the standard methodology.

The thesis is meant to be created in partnership with Garrett Motion Czech Republic s.r.o. The results should contribute to the development of a new tool for turbocharger performance maps management and post-processing.

## INTRODUCTION

Turbocharged combustion engines represent, as of today, the main building block of most road vehicle powertrains. Ranging from the smallest to the largest, they can be found in all passenger and freight means of transport, as well as off-highway and stationary applications. In the context of increasing climate protection efforts, it is of great importance to sustain continuous improvement of our technologies. This is only made possible by means of accurate simulation tools, which allow engineers to predict the impact of their innovative ideas.

Modelling of turbocharger performance is an important part of the development of internal combustion engines. Although working solutions are integrated in existing commercial software to enable simulations of boosted engine working cycles, tools for post-processing of measured or CFD predicted data are less common. Therefore, the main objective of this work is to develop an application that will allow engineers to visualize and compare the performance of different turbine stages. However, the trade-offs between efficiency and corrected mass flow rate must be studied at equal operating conditions, which requires the scattered input data to be fitted by a convenient mathematical model.

Since the goal behind a turbine stage selection is to use its characteristics in engine performance simulations, it would be advantageous to apply the same turbine model for both purposes (to avoid any distortion caused by differences in data pre-processing). Therefore, in this work, the turbine fitting method integrated in GT-SUITE™ is studied. On that basis, a new algorithm is proposed, the objective of which is to further improve the fidelity of turbine performance extrapolation while maintaining the robustness and flexibility of the existing process. This is achieved by implementing physics principles to constrain some aspects of the model, the properties of which are identified with the help of optimization.

MATLAB™ is selected as the development environment for the intended application because it is suitable for both functional coding and graphical user interface design. In addition, an SQLite database is used as storage for raw measured data and fitted models to facilitate database operations such as searching, filtering, or aggregation. An export function is integrated to enable the generation of fully extrapolated turbine maps that can be imported into engine simulation software (in the so-called *grid* format in the case of GT-SUITE).

The new methodology is validated by evaluating turbine performance trends that are generated with the help of up to 53 fitted gas stand maps. Also, engine performance is simulated to check for any differences between the results obtained using the default and proposed turbine fitting methods.

# 1 TURBOCHARGING

Turbocharging is the name of a method used to increase the power density of internal combustion engines. This is accomplished by forced induction, the effect of which is an increase in the intake air density. Because of that, engines can burn more fuel and produce more power at the same operating speed and with the same displacement volume. This process is commonly referred to as downsizing, because it enables a smaller engine to produce the same amount of power as a larger naturally aspirated counterpart. A common turbocharger consists of a turbine and a compressor, both of which are mounted on the same shaft (see Figure 1).

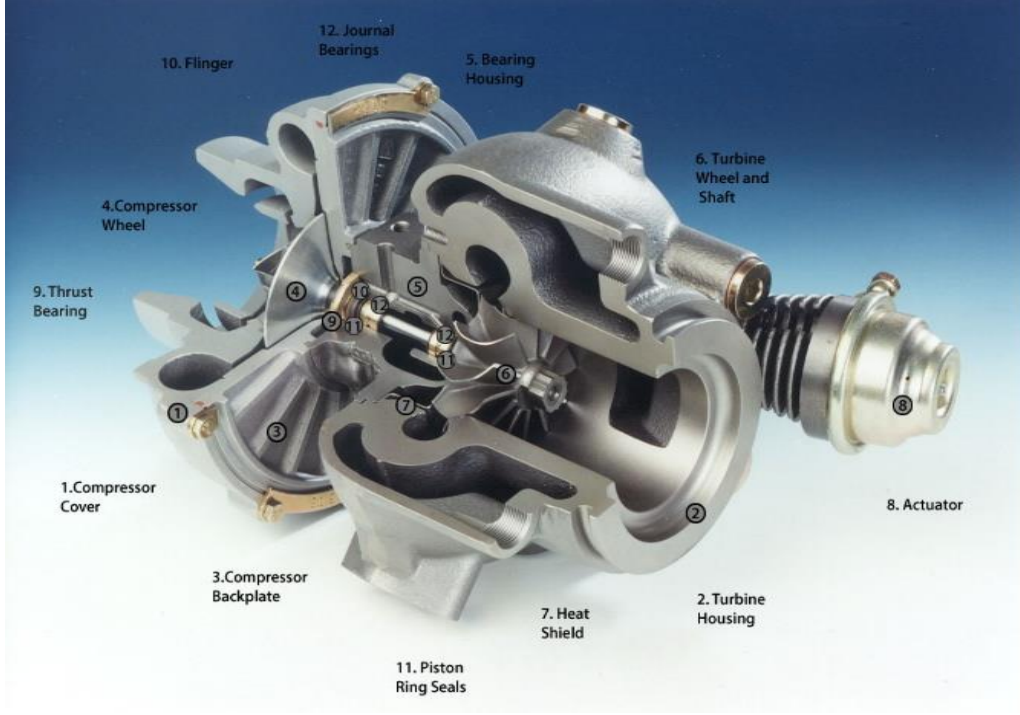


Figure 1: Turbocharger section view [21]

Engine power is directly proportional to the amount of fuel that is burned per unit of time. This is a process in which chemical energy is transformed into mechanical energy. However, complete combustion is only possible when the available amount of air is at least as high as stoichiometric (i.e. it enables the oxidation of all carbon and hydrogen atoms in the fuel). Therefore, the theoretical engine power output depends on the intake air mass flow rate in the following way [1, 3, 5]

$$P_e = \eta_e \dot{m}_{air} \frac{H_u}{L_t \lambda} \quad (1)$$

where  $P_e$  [W] is the engine brake power,  $\eta_e$  [-] is the overall engine efficiency,  $\dot{m}_{air}$  [kg/s] is the air mass flow rate,  $H_u$  [J/kg] is the fuel lower heating value,  $L_t$  [-] is the stoichiometric ratio (given by the chemical composition of each fuel) and  $\lambda$  [-] is the air excess ratio. It is common that petrol engines (spark-ignited) are operated mostly close to the stoichiometric conditions, whereas diesel engines (compression-

ignited) are always running lean (with air excess). The average air mass flow rate through a piston engine can be expressed as [1, 2, 3]

$$\dot{m}_{air} = \eta_v \rho_{int} V_d \frac{n_e}{60\tau} \quad (2)$$

where  $\eta_v$  [-] is the volumetric efficiency,  $\rho_{int}$  [kg/m<sup>3</sup>] is the intake air density,  $V_d$  [m<sup>3</sup>] is the total cylinder displacement,  $\tau$  [-] is the number of crankshaft revolutions per one engine cycle (a four-stroke engine needs two revolutions) and  $n_e$  [1/min] is the engine speed. Volumetric efficiency can be determined either experimentally or by simulation (e.g., using 1D engine gas dynamics software). The intake air density depends on pressure and temperature, as described by the ideal gas equation of state [1, 2, 3, 5, 9]

$$\rho_{int} = \frac{p_{int}}{r_{air} T_{int}} \quad (3)$$

where  $p_{int}$  [Pa] is the intake air pressure,  $r_{air}$  [J/(kg·K)] is the specific gas constant and  $T_{int}$  [K] is the intake air temperature. The latter increases during compression, so a common practice is to cool the flow down in a heat exchanger (see Figure 2). The power needed to drive the compressor is generated by the turbine, which is propelled by exhaust gases created as a product of combustion in the engine. Transfer of mechanical power is performed by a shaft. [2, 3, 5]

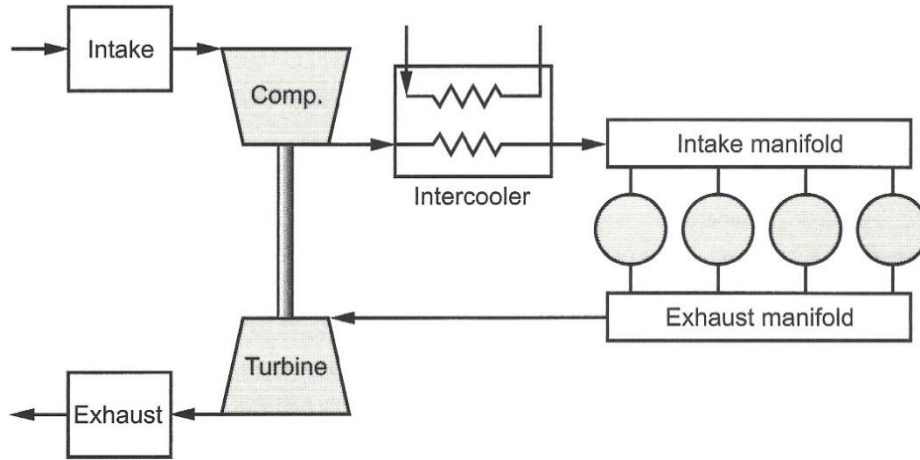


Figure 2: Turbocharged engine gas flow scheme [3]

Piston engines operate with an intermittent working cycle, which is followed by strong pulsations in the exhaust system upstream of the turbine (see Figure 3). With the opening of the exhaust valves, the instantaneous pressure and temperature increase rapidly in the ports and propagate further in the form of a pressure wave. Subsequent expansion in a turbine makes the pressure in the exhaust manifold fall again until the next event begins. The entire process is repeated with a frequency corresponding to the engine speed and the number of attached cylinders. Furthermore, the longer the period, the more time is available for the gas to exit through the turbine, which results in higher pressure amplitude. This situation is typical for turbocharging of engines



with a low number of cylinders (three or less). On the contrary, a higher number of cylinders (four or more) results in a more stable turbine operation during one engine working cycle. [2, 3]

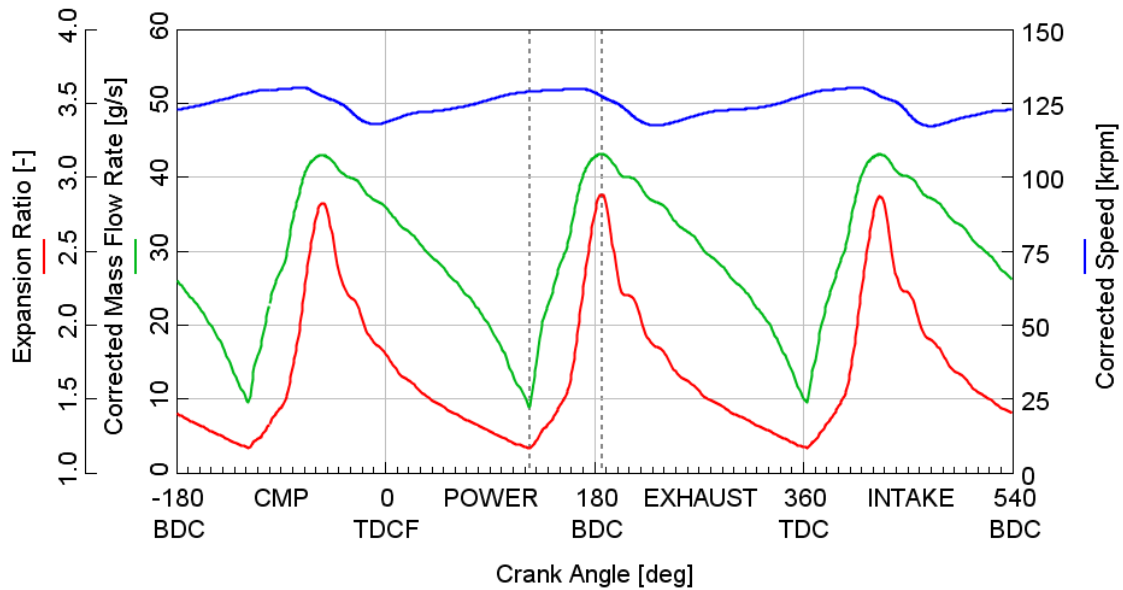


Figure 3: Small three-cylinder engine working cycle simulation in GT-SUITE<sup>TM</sup> (TDCF – top dead centre firing, TDC – top dead centre, BDC – bottom dead centre)

While the expansion ratio follows the pulsating inlet pressure, the rotor speed changes only a little due to its inertia (see Figures 16 & 17). It means that to enable a turbocharged engine gas dynamics simulation, turbine performance must be defined over a wide range of expansion ratio at each speed line. That is, however, in a large contrast to what can be captured by a hot gas stand (see Figure 4).

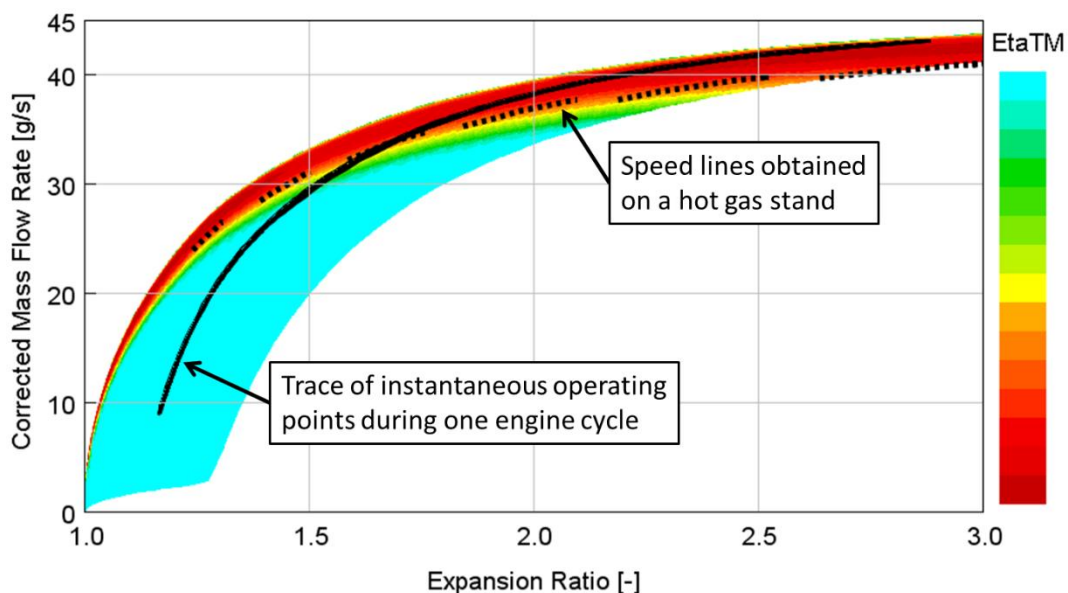


Figure 4: Turbine corrected mass flow rate map with a trace of instantaneous operating points during one engine cycle simulated in GT-SUITE

## 2 BASELINE TURBINE FITTING METHOD

The main goal of this work is to develop an application that will facilitate pre-processing and comparison of turbine maps. To study the trade-offs at equal operating conditions, however, measured data must be fitted by a mathematical model. Since the same is required to enable turbocharged engine working cycle simulations, it would be advantageous to use one turbine model for both purposes. Therefore, the turbine fitting method integrated in GT-SUITE is studied to set a baseline. However, this process is not exhaustively documented in available information sources, so custom procedures had to be proposed where necessary (see [10, 20]).

### 2.1 PRE-PROCESSING OF INPUT DATA

The first step of the baseline turbine fitting method is to group the measured operating points into speed lines (the standard mapping at constant speeds is assumed). An operating point with the highest efficiency is identified at each speed line of the sample gas stand map and its index is saved for later use (see Figure 5).

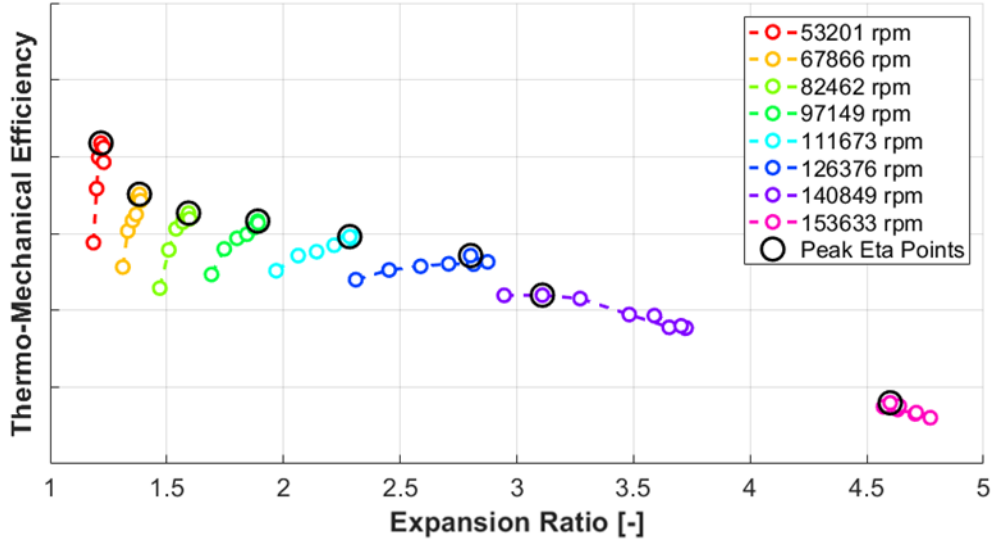


Figure 5: Identification of speed lines and maximum-efficiency points

### 2.2 FITTING THE OPTIMUM BLADE SPEED RATIO

Blade speed ratio ( $BSR$ ) is defined as a ratio between the circumferential velocity of a turbine wheel and the isentropic spouting velocity [2, 3, 4, 5]

$$BSR = \frac{u}{c_0} = \frac{\pi D_T \frac{n_{TC}}{60}}{\sqrt{2c_{p_{exh}}T_{1T_{tot}} \left[ 1 - \left( \frac{p_{2T}}{p_{1T_{tot}}} \right)^{\frac{\gamma_{exh}-1}{\gamma_{exh}}} \right]}} \quad (4)$$

where  $BSR$  [-] is the blade speed ratio,  $u$  [m/s] is the turbine circumferential velocity,  $c_0$  [m/s] is the isentropic spouting velocity,  $D_T$  [m] is the wheel diameter,  $n_{TC}$  [1/min] is the turbocharger speed,  $c_{p_{exh}}$  [J/(kg·K)] is the specific heat capacity

at constant pressure,  $T_{1T\_tot}$  [K] is the inlet total temperature,  $p_{1T\_tot}$  [Pa] is the inlet total pressure,  $p_{2T}$  [Pa] is the outlet static pressure and  $\gamma_{exh}$  [-] is the ratio of specific heat capacities (the index *exh* indicates burnt gas). The optimum blade speed ratio ( $BSR_{opt}$ ) is such a value of  $BSR$  that enables reaching the maximum turbine efficiency at certain level of expansion ratio ( $PRT$ ; see Chapter 2.1 and Figure 6).

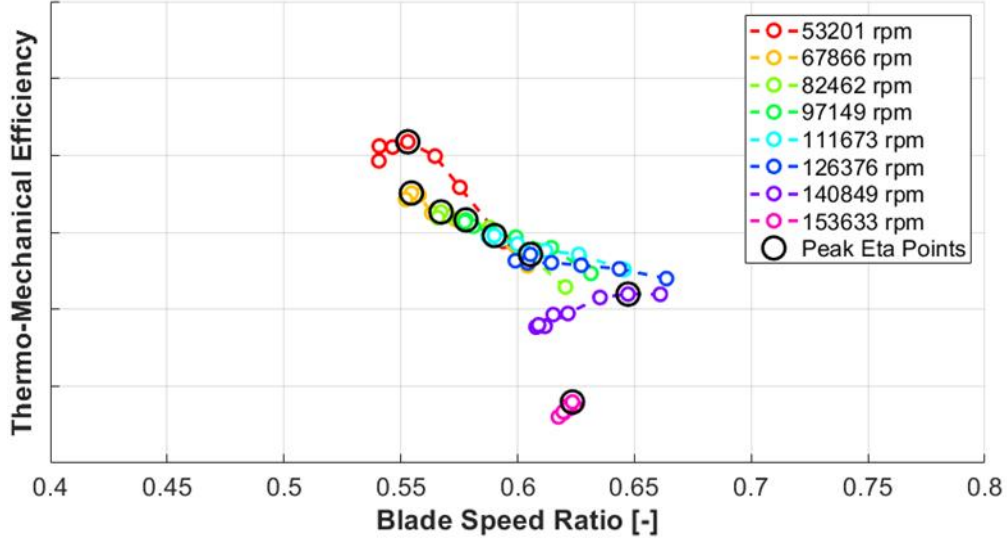


Figure 6: Efficiency vs.  $BSR$  with highlighted maximum-efficiency points

The relationship between  $BSR_{opt}$  and  $PRT$  is supposed to be linear according to the available information sources [10, 20]

$$BSR_{opt} = kPRT + q \quad (5)$$

where  $BSR_{opt}$  [-] is the optimum blade speed ratio,  $k$  [-] is the slope and  $q$  [-] the elevation of the fitted line. Constants  $k$  and  $q$  are determined using linear least squares regression of the optimum operating points identified during the input data pre-processing (see Chapter 2.1 and Figures 6 & 7).

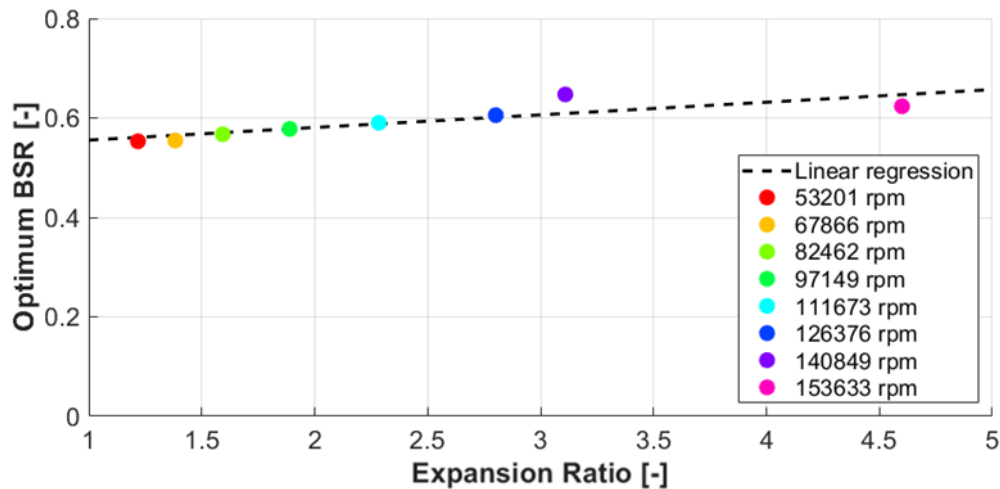


Figure 7: Linear regression of the optimum blade speed ratio

As soon as the characteristic function for  $BSR_{opt}$  is known, normalized blade speed ratio ( $BSR_{norm}$ ) can be calculated at each operating point of the measured map.  $BSR_{norm}$  is defined as the ratio between the  $BSR$  at given operating point and the optimum  $BSR$  at the same level of  $PRT$  [10, 20]

$$BSR_{norm} = \frac{BSR}{BSR_{opt}} \quad (6)$$

### 2.3 FITTING THE MAXIMUM EFFICIENCY

The maximum-efficiency points identified at each speed line during the pre-processing of a turbine map (see Chapter 2.1) are fitted with respect to corrected speed. However, no particular function is suggested in the available information sources (except that it should be smooth; see [10, 20]). A spline curve can be recommended for its stability and easy definition of extrapolation modes (due to its piecewise polynomial form). As a conservative strategy, flat extrapolation is applied, which is also the default option in GT-SUITE (see Figure 8).

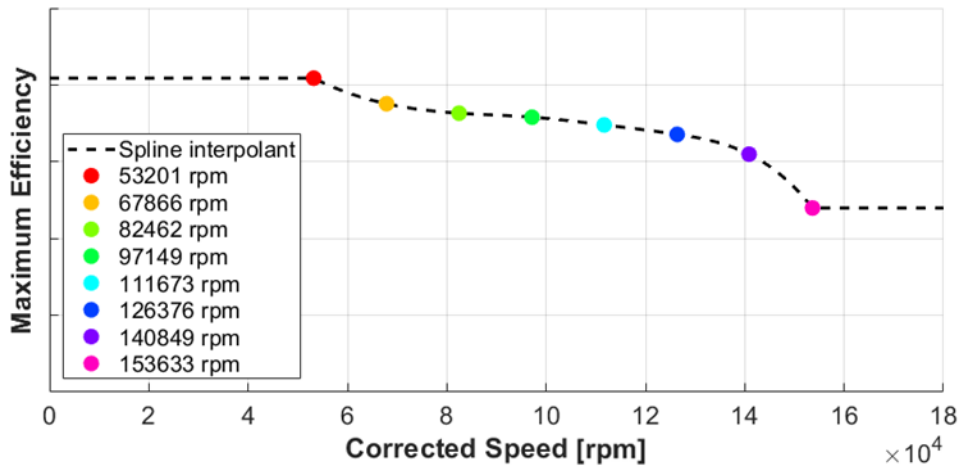


Figure 8: Maximum turbine efficiency as a cubic spline with flat extrapolation

Once the characteristic function for maximum efficiency is available, the normalized efficiency can be calculated at each operating point of the map. Normalized efficiency ( $ETATM_{norm}$ ) is defined as a ratio between the efficiency at given operating point ( $ETATM$ ) and the maximum efficiency at the same level of expansion ratio ( $ETATM_{max}$ ) [10, 20]

$$ETATM_{norm} = \frac{ETATM}{ETATM_{max}} \quad (7)$$

The maximum efficiency function is, however, defined relative to corrected speed, so the optimum corrected speed ( $NT_{opt}$ ) at given expansion ratio must be found at each operating point first. To do that, the  $BSR_{opt}$  function (see Equation 5) must be combined with the definition of  $BSR$  (see Equation 4). Also, reference gas properties must be used, so that corrected speed is obtained ( $T_{1T_{ref}} = 288 \text{ K}$ )

$$NT_{opt} = (kPRT + q) \frac{\sqrt{2c_{p\_exh} T_{1T\_ref} \left[ 1 - \left( \frac{1}{PRT} \right)^{\frac{\gamma_{exh}-1}{\gamma_{exh}}} \right]}}{\frac{\pi D_T}{60}} \quad (8)$$

## 2.4 FITTING THE NORMALIZED EFFICIENCY

All turbine operating points should lie on a single curve in the normalized efficiency versus normalized blade speed ratio diagram. In GT-SUITE, the fitting function has two parts. For  $BSR_{norm} < 1$ , exponentiation is used [10, 20]

$$ETATM_{norm} = 1 - (1 - BSR_{norm})^{b_{fit}} \quad (9)$$

where  $b_{fit}$  [-] is the fitted parameter. The other part of the normalized efficiency curve, where  $BSR_{norm} \geq 1$ , is fitted by a parabola [10, 20]

$$ETATM_{norm} = 1 - c_{fit}(BSR_{norm} - 1)^2 \quad (10)$$

where  $c_{fit}$  [-] is the fitted parameter. The value of  $BSR_{norm}$ , at which the  $x$ -axis is crossed, can be determined using an equation

$$BSR_{norm\_ETA\_int} = \frac{1}{c_{fit}^2} + 1 \quad (11)$$

The complete curve of normalized efficiency is anchored to a point with coordinates [1,1]. It can be interpreted as a generalized optimum that the turbine works with the highest efficiency at (see Figure 9).

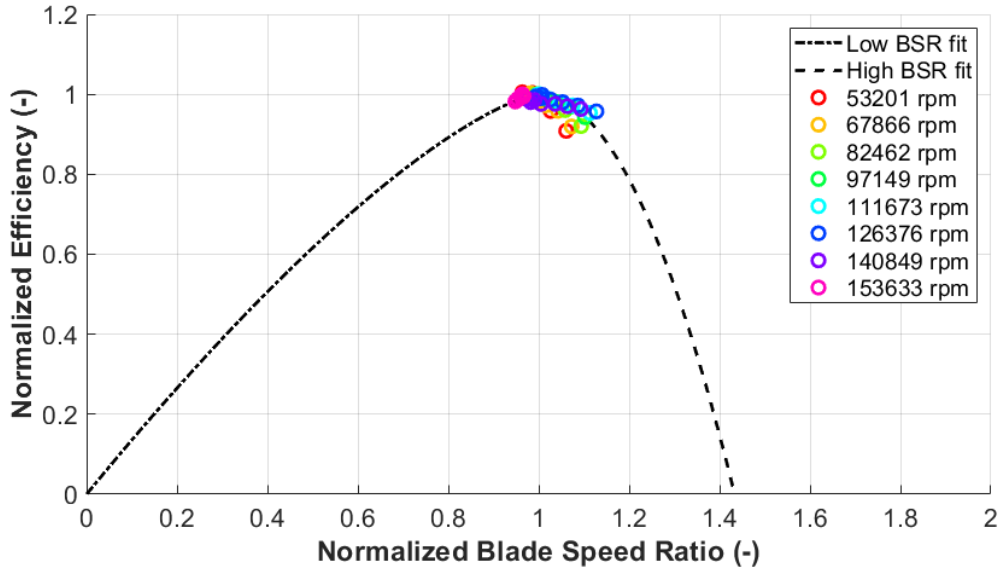


Figure 9: Normalized efficiency versus normalized blade speed ratio

## 2.5 FITTING THE OPTIMUM CORRECTED MASS FLOW RATE

Optimum corrected mass flow rate is associated with the operating points of maximum efficiency at each speed line (see Chapter 2.1). It is fitted with respect to

corrected speed, for which a spline curve is recommended like in the case of the maximum efficiency function (see Chapter 2.3). Flat extrapolation is applied in the direction of high corrected speeds only, since the function must pass through the origin of coordinates.

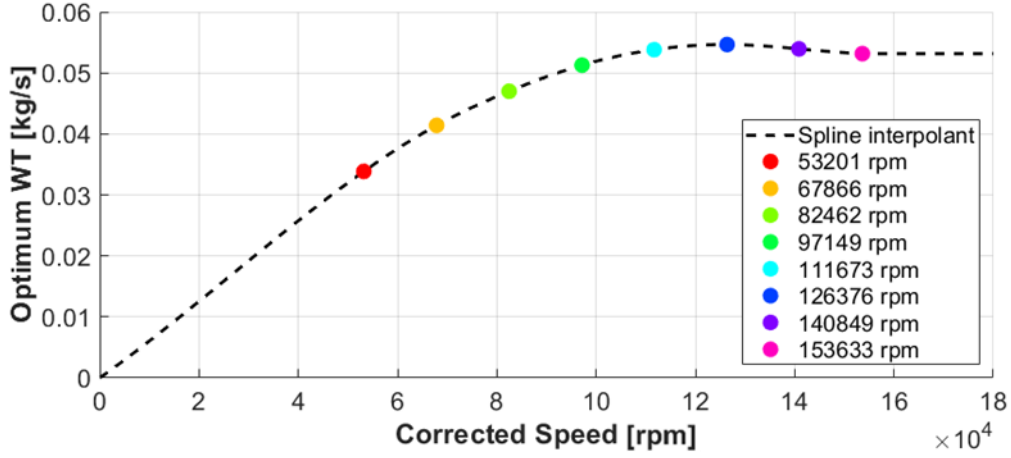


Figure 10: Optimum corrected mass flow rate spline with flat extrapolation

With the characteristic function for optimum corrected mass flow rate ( $WT_{opt}$ ) available, normalized mass flow rate ( $WT_{norm}$ ) can be calculated at each operating point of the map.  $WT_{norm}$  is defined as a ratio between the corrected mass flow rate at given operating point ( $WT$ ) and the optimum corrected mass flow rate at the same level of expansion ratio [10, 20]

$$WT_{norm} = \frac{WT}{WT_{opt}} \quad (12)$$

Similarly to the case of the maximum efficiency function (see Chapter 2.3), the characteristic function for  $WT_{opt}$  is defined with respect to corrected speed, so the optimum corrected speed at each expansion ratio must be found using Equation 8 first.

## 2.6 FITTING THE NORMALIZED MASS FLOW RATE

All turbine operating points should lie on a single curve in the normalized mass flow rate versus normalized blade speed ratio diagram. In GT-SUITE, the fitting function is exponentiation in the form [10, 20]

$$WT_{norm} = c_m + BSR_{norm}^{m_{fit}}(1 - c_m) \quad (13)$$

where  $c_m$  [-] and  $m_{fit}$  [-] are fitted parameters. The constant  $c_m$  determines the value of  $WT_{norm}$  at zero  $BSR_{norm}$  (the intercept with the y-axis, see Figure 11). Similarly, the exponent  $m_{fit}$  controls the curvature of the fitting function and thus the intercept with the x-axis. The latter can be enumerated using an expression

$$BSR_{norm\_WT\_int} = \left( \frac{c_m}{c_m - 1} \right)^{\frac{1}{m_{fit}}} \quad (14)$$

where  $BSR_{norm\_WT\_int}$  [-] is the value of  $BSR_{norm}$  at the intercept. It should be noted that normalized mass flow rate usually reaches zero at a much higher value of  $BSR_{norm}$  compared to normalized efficiency (see Figures 9 & 11).

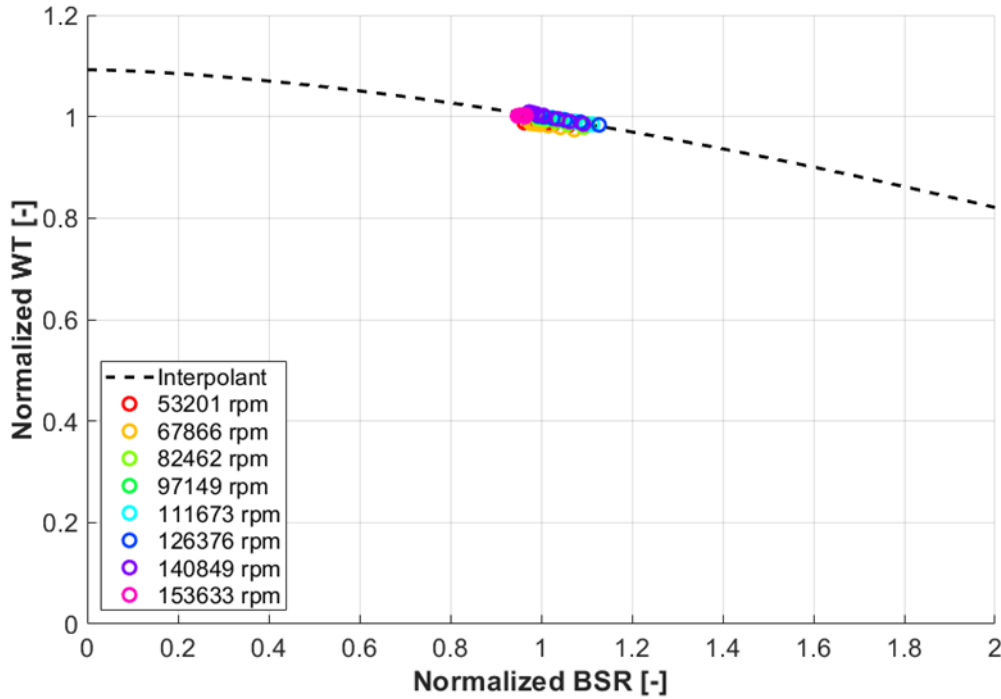


Figure 11: Normalized mass flow rate versus normalized blade speed ratio

## 2.7 OPTIMIZATION

Until now, the properties of the baseline turbine model were explicitly defined by the input map data. However, operating points of the maximum efficiency, which are key to the fitting process, are generally not included among the outputs of a measurement (e.g. hot gas stand). Therefore, it is advantageous to apply optimization methods to identify these relationships.

The function of optimum blade speed ratio versus expansion ratio is central to the turbine model. As it is linear, there are only two independent parameters to calibrate (see Equation 5). The simplex method can be recommended for this purpose with the properties of the initial non-optimized fit as the starting point.

The second aspect of the turbine model, that is influenced by the identification of optimum operating points, is the maximum efficiency spline. The simplex method can be applied to determine the y-coordinate of each break-point in such a way that the root-mean-square error between the input map data and the model is minimized.

A similar process is followed with the optimum corrected mass flow rate spline, while the properties of the initial non-optimized fit are used as the optimization starting point. The resulting fully extrapolated efficiency map (representative of the sample data obtained on a hot gas stand) is shown in Figure 12. It can be noted that the maximum efficiency curve is located further away from the data points of the highest speed line now (after the optimization). Nevertheless, the overall fit quality is good (the root-mean-square error is 0.71%).



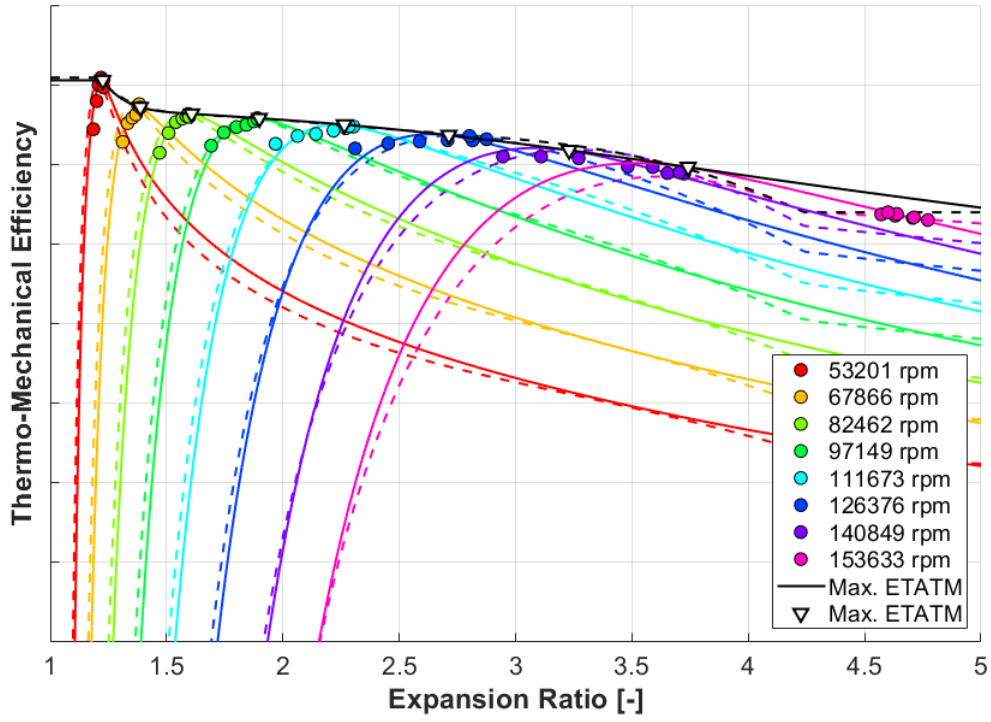


Figure 12: Fully extrapolated efficiency map at the end of the baseline turbine fitting process (full lines) and the initial non-optimized one (dashed)

The fully extrapolated corrected mass flow rate map is included in Figure 13. In this case, however, a significant distortion can be recognized at low expansion ratios, where the speed lines should be more spread due to the effect of centrifugal forces.

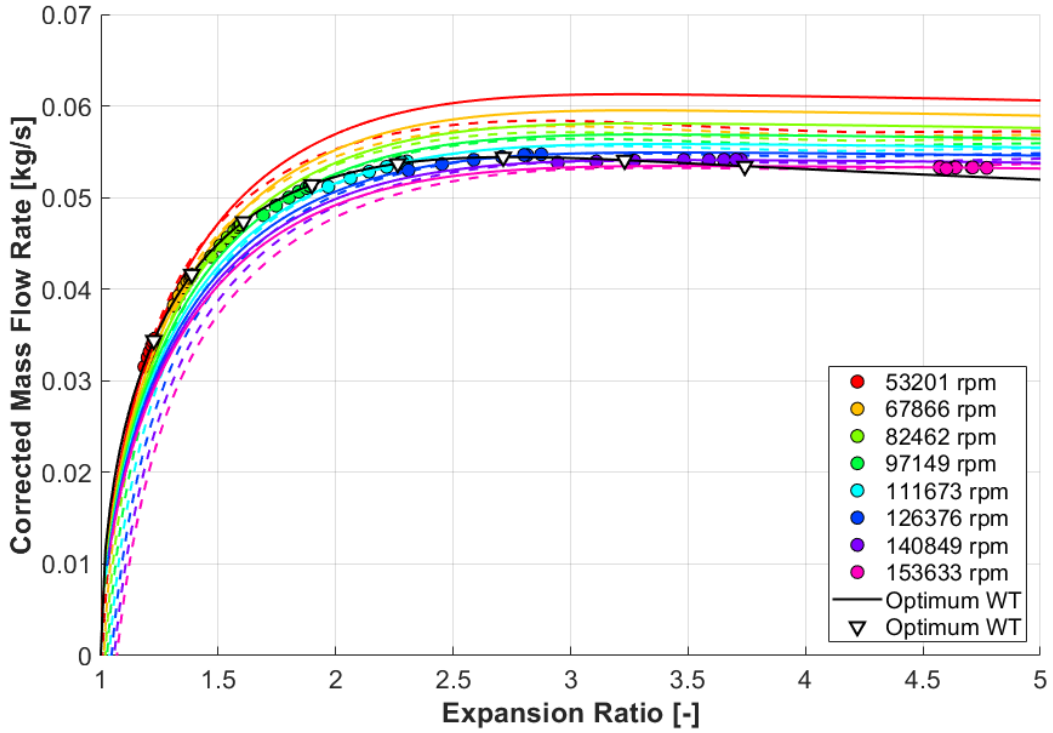


Figure 13: Fully extrapolated mass flow rate map at the end of the baseline turbine fitting process (full lines) and the initial non-optimized one (dashed)



### 3 NEW TURBINE FITTING ALGORITHM

With the new turbine fitting algorithm, emphasis is placed on the implementation of physics principles to improve the quality of extrapolation. In line with the observations introduced in Chapter 2.7 (see the condensed speed lines at low expansion ratios in Figure 13), the theory of radial equilibrium is applied to model the effect of centrifugal forces on the corrected mass flow rate.

#### 3.1 RADIAL EQUILIBRIUM

At zero mass flow rate, the turbine inlet pressure must be in equilibrium with the centrifugal force acting on the fluid enclosed in the rotating blade channels. The corresponding pressure ratio depends on the speed of rotation as [11]

$$\frac{p_2}{p_1} = \left[ 1 + \frac{\gamma_{exh} - 1}{2\gamma_{exh}} \frac{1}{r_{exh} T_{1T_{ref}}} \left( \frac{\pi NT}{30} \right)^2 (R_{2\_RMS}^2 - R_{1\_RMS}^2) \right]^{\frac{\gamma_{exh}}{\gamma_{exh} - 1}} \quad (15)$$

where  $R_{2\_RMS}$  [m] is the bigger mean-flow radius and  $R_{1\_RMS}$  [m] is the smaller mean-flow radius. This can be used to calculate the expansion ratio at the intercept of each speed line with the x-axis in a corrected mass flow rate map (see Figure 13). Consequently, the exponent  $m_{fit}$  of the normalized mass flow rate function can be pre-determined and used as a constraint during the fitting process (see Chapter 2.6).

#### 3.2 IDEAL NOZZLE ANALOGY

Another feature of the turbine model, which needs to be improved, is the slope of the optimum corrected mass flow rate at high expansion ratios. In the baseline method, the shape of the corresponding spline part is determined only by the location of the nearest measured operating points (such that fit error is minimized). However, it can be pointed out that the flow through a turbine stage should reach saturation at a certain expansion ratio, which is commonly referred to as choke. Under such conditions, the corrected mass flow rate cannot increase further, because the speed of sound has been achieved in the critical flow cross section. This can be illustrated by a formula for the corrected mass flow rate derived from the expression for the critical mass flow rate through an ideal nozzle (see [9])

$$\dot{m}_{0\_corr\_crit} = \sqrt{2c_p \left[ 1 - \beta_{crit}^{\frac{\gamma-1}{\gamma}} \right]} A_n \frac{1}{r} \beta_{crit}^{\frac{1}{\gamma}} \frac{p_{ref}}{\sqrt{T_{ref}}} \quad (16)$$

where  $\beta_{crit}$  [-] is the critical expansion ratio (constant at choke),  $r$  [J/(kg·K)] is the specific gas constant.

At zero wheel speed there is no centrifugal force to further influence the balance of pressures, so the corresponding corrected mass flow rate should stay constant at choke. According to the definition of normalized mass flow rate function (see Equation 13), the corrected mass flow rate at zero wheel speed is proportional to the

optimum corrected mass flow rate. Therefore, it can be concluded that the optimum corrected mass flow rate should stay constant under choke conditions as well.

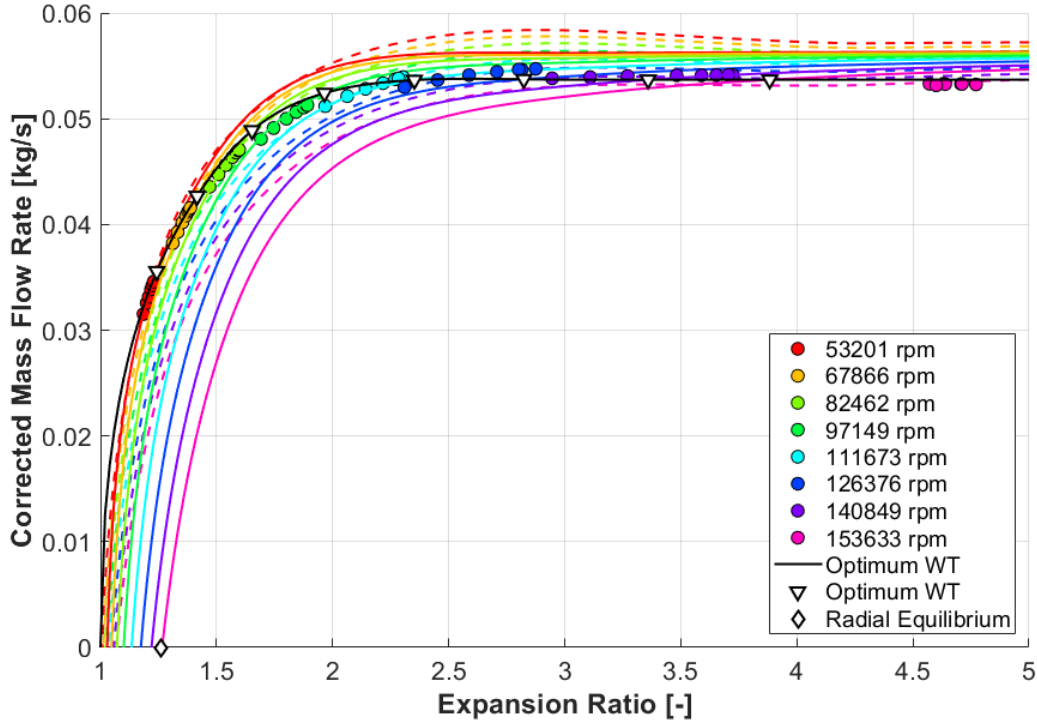


*Figure 14: Extrapolation of corrected mass flow rate with non-decreasing optimum corrected mass flow rate function*

Based on the analysis of the fully extrapolated corrected mass flow rate map in Figure 14, it can be concluded that the fit quality at low expansion ratios has improved thanks to the introduction of the theory of radial equilibrium. Measured operating points at the highest speed line are, however, no longer fitted with the new constraint of constant optimum corrected mass flow rate at choke. At the same time, the extrapolated speed lines are rather condensed in this area, which is not a desired state, because the corrected mass flow rate should decrease with increasing spinning speed due to the centrifugal forces.

The reason behind this behaviour is that the linear optimum blade speed ratio function increases with the expansion ratio, which implies the same trend of the optimum corrected speed too (see Figure 7). Therefore, every speed line must cross the optimum corrected mass flow rate at some expansion ratio. Since the optimum corrected mass flow rate is constant at choke, all non-zero speed lines are monotonically increasing and getting closer to each other with increasing expansion ratio. That is, however, in contradiction to the measurement. Furthermore, if the theory of radial equilibrium were assumed to approximate the centrifugal effect at non-zero mass flow rates, it would imply that the offset with respect to expansion ratio is independent of turbine inlet pressure (see Equation 15) and all speed lines should be parallel at choke. The only way all these constraints can be satisfied at the same time is by keeping the optimum corrected speed constant under choke conditions.

### 3.3 OPTIMUM CORRECTED SPEED LIMITATION

From the perspective of turbine aerodynamics, it is assumed that the wheel-inlet flow velocity and the absolute flow angle (in stationary frame of reference) are independent of the expansion ratio at choke. Therefore, it can be concluded that the highest efficiency is achieved at such a circumferential wheel speed, which results in the most convenient relative flow angle at the leading edge of the turbine blades. For this reason, the idea of optimum corrected speed limitation at choke appears feasible.

Since the optimum corrected turbine speed is derived from the optimum blade speed ratio, the corresponding characteristic function must be adapted to enable the required limitation. At this point, it should be emphasized that blade speed ratio is defined as a ratio between the circumferential velocity of the wheel and the isentropic spouting velocity (see Equation 4). However, the latter is constant under choke conditions, which must be reflected in the procedure of calculating the blade speed ratio at every operating point of the input map (see Chapter 2.2). Also, it implies that optimum blade speed ratio must stay constant to produce the constant optimum corrected speed at choke. Nevertheless, the corresponding spline must be tangent to a constant corrected speed curve at the choke point in the optimum blade speed ratio versus expansion ratio diagram to avoid sharp transitions (see Figure 15).

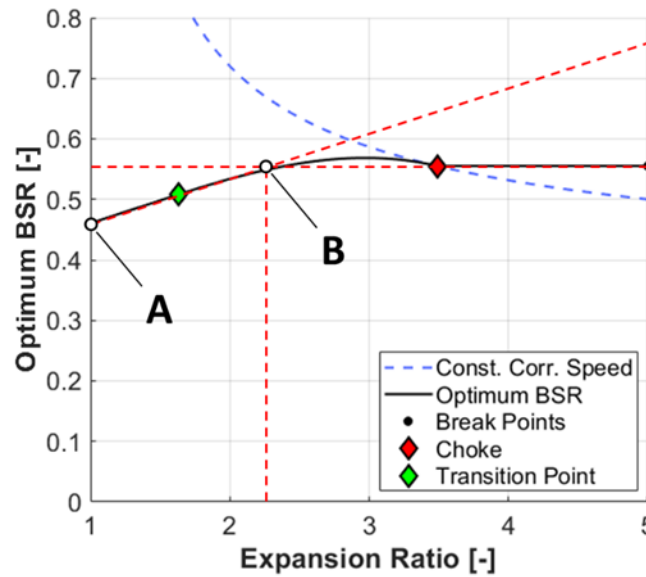


Figure 15: Optimum blade speed ratio spline

It can be noted that the optimum blade speed ratio spline retained its linear character at low expansion ratios (see the section between the point A and the transition point in Figure 15). This part is fitted to the input data in the same way as the complete linear function in the baseline algorithm (two-parametric optimization). The middle section, located between the transition point and the choke point, is a cubic polynomial with prescribed end-slopes (taken over from the adjacent spline parts). Finally, the flat section at high expansion ratios is fully defined by the choke point, the location of which is determined by a dedicated optimization process. As an important consequence of optimum corrected speed limitation, there is no optimum expansion

ratio associated with the speed lines above the choke speed limit, so they cannot intersect with the maximum efficiency curve (see Figure 16).

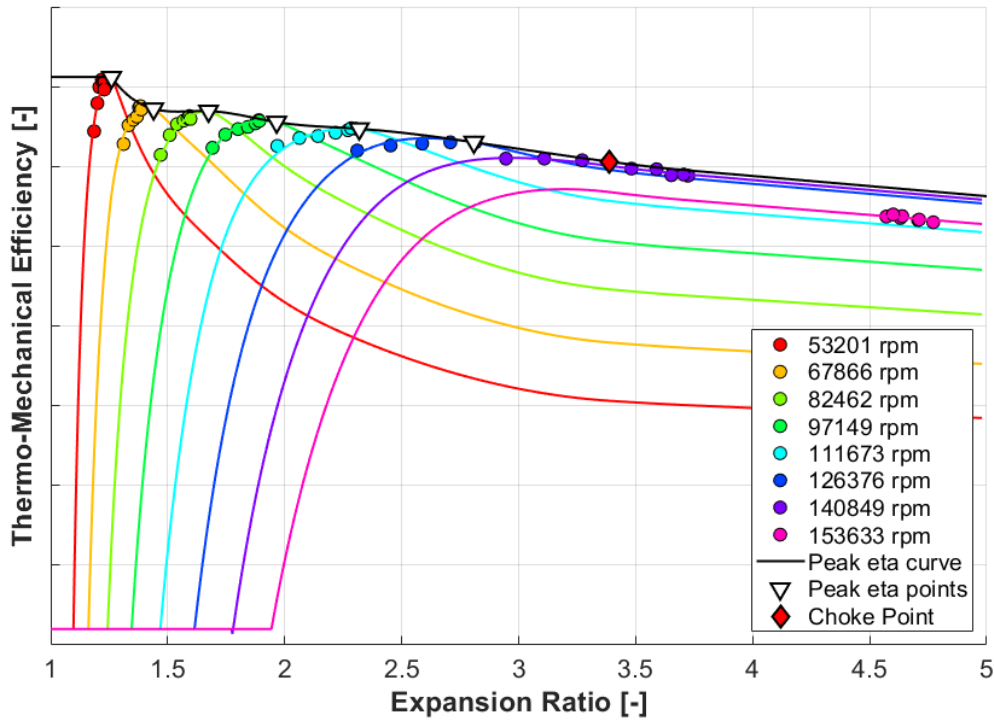


Figure 16: Fully extrapolated efficiency map with the optimum BSR limitation

The new method was successful in modelling the turbine efficiency (the root-mean-square error is 0.43%). Also, the criteria for the quality of the corrected mass flow rate extrapolation are now fulfilled (see Figure 17; the root-mean-square error is 0.16%).

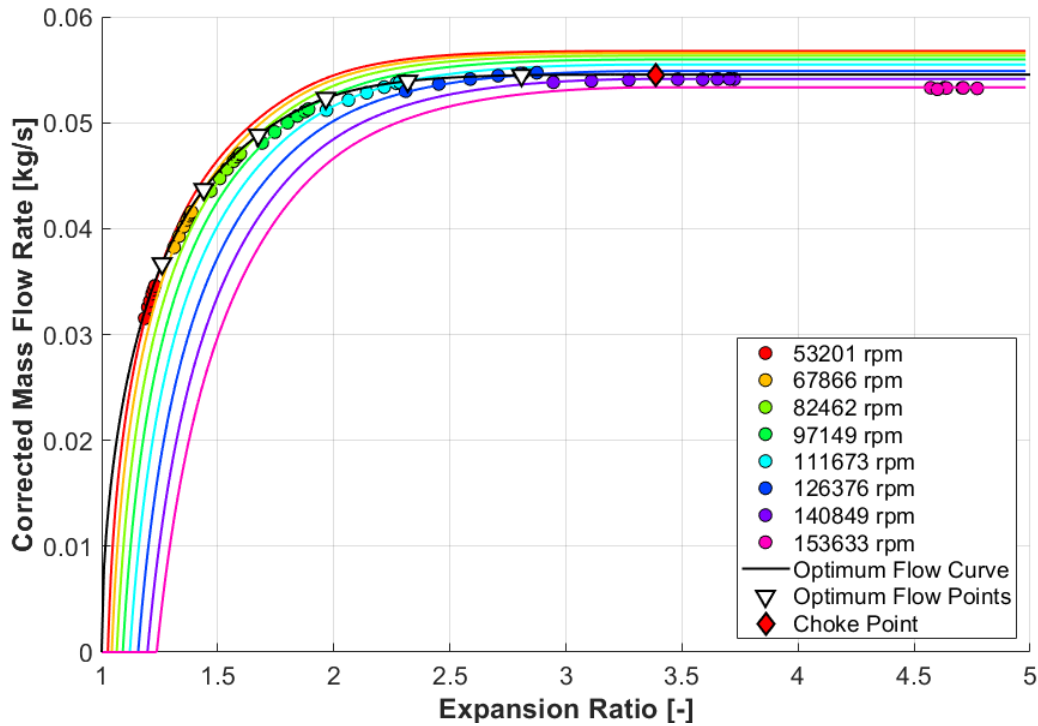


Figure 17: Fully extrapolated mass flow map with the optimum BSR limitation

## 4 VALIDATION OF THE PROPOSED METHODOLOGY

The developed MATLAB application is equipped with an SQLite 3 database to store both raw measured data and fitted turbine models, which proved to be advantageous in multiple ways (see [25]). The interface is shown in Figure 18.

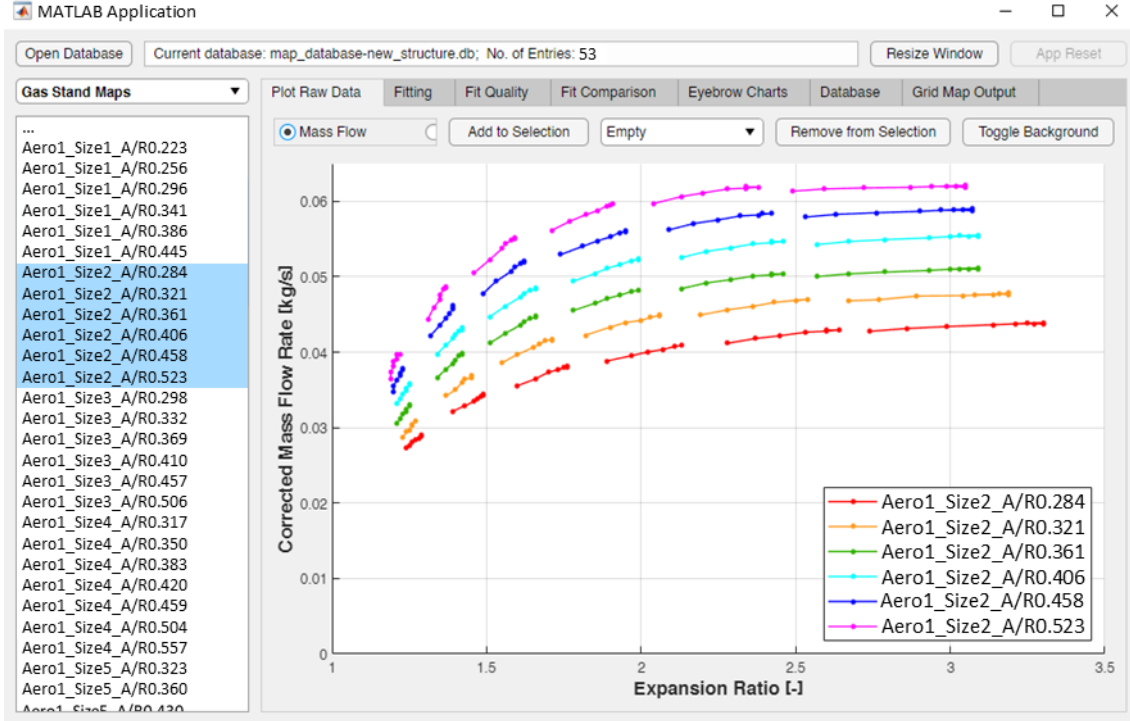


Figure 18: Raw corrected mass flow rate linked to the selected database entries

Fitted models can be used to plot performance trends that span multiple turbine stages of varying properties. An important relationship of this type is between the maximum efficiency and the optimum corrected mass flow rate at a certain expansion ratio for a range of volute sizes at a constant wheel diameter (see Figure 19).

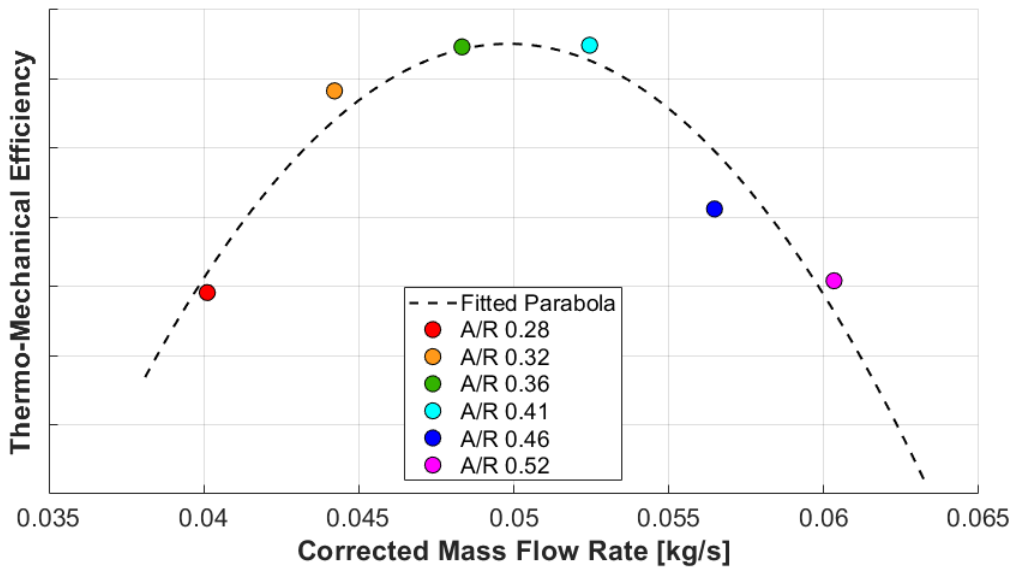


Figure 19: Maximum efficiency vs. corrected mass flow rate at  $PRT = 2$

After the relationship between the maximum turbine efficiency and the volute size has been resolved (the so-called eyebrow), the chart can be extended to cover a range of wheel diameters. This is sometimes referred to as the size effect (see Figure 20).

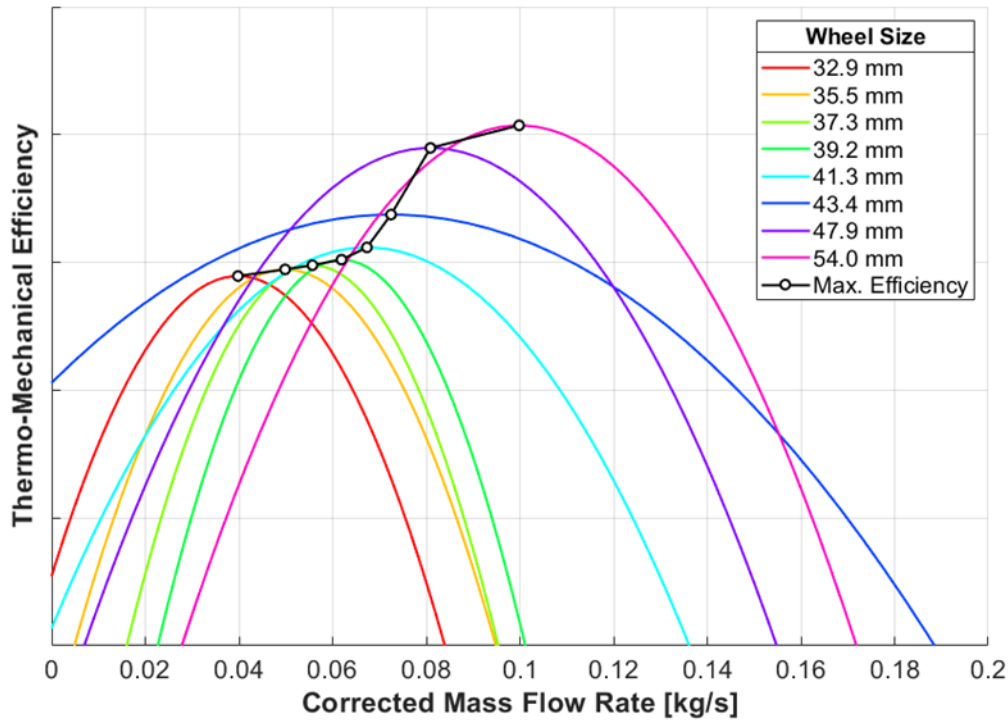


Figure 20: Composition of eyebrow charts generated at the expansion ratio two for a range of turbine sizes sharing the same wheel aerodynamic design

It can be concluded that the proposed turbine fitting methodology is robust enough to enable plotting of valid performance trends related to the effects of wheel and volute sizes (see Figures 19 & 20; source data was obtained on a hot gas stand).

#### 4.1 ENGINE PERFORMANCE SIMULATION – STEADY STATE

To evaluate the effects of differences in the turbine model, engine performance was simulated using both the GT-SUITE default and the proposed fitting methods.

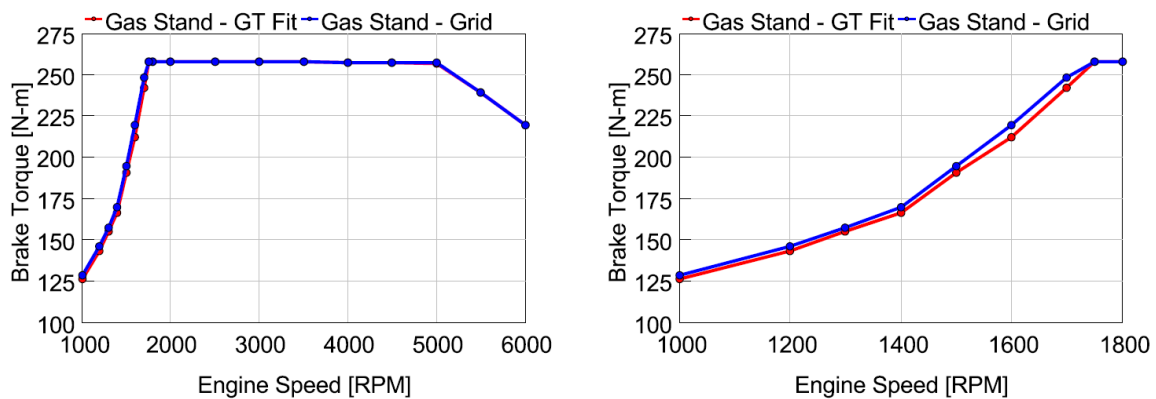


Figure 21: Full load simulation with fitted turbine maps obtained by a hot gas stand measurement (*red* – the default fit, *blue* – the proposed algorithm)

The biggest difference in full-load performance with the gas stand map can be observed at 1600 rpm, where the default fit gives by 7 Nm lower brake torque compared to the proposed algorithm (see Figure 21). That corresponds to an approximately 3% offset, which can be considered a good agreement between the two models. At higher engine speeds, the boost pressure is controlled by the wastegate.

The same simulation was repeated with an equivalent map obtained on a turbine dynamometer. The trade-off between the fitting methods is shown in Figure 22.

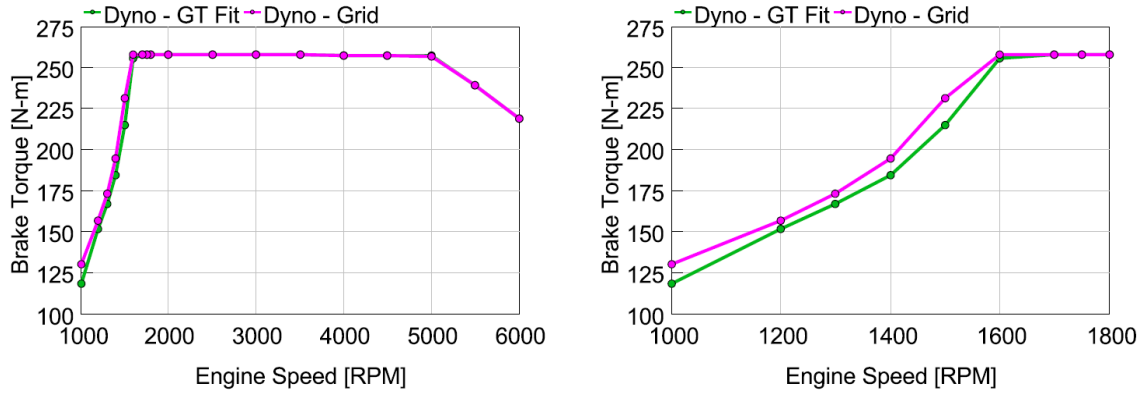


Figure 22: Full load simulation with fitted turbine maps obtained by a dynamometer measurement (*green* – the default fit, *pink* – the proposed algorithm)

The impact of the fitting method on the achievable low-end torque is bigger with the dyno map (see Figures 21 & 22). At 1500 rpm, the difference is as high as 16.5 Nm or 7.7%. Such a gap is already significant.

## 4.2 ENGINE PERFORMANCE SIMULATION – TRANSIENT

Engine dynamics is usually evaluated in terms of torque response to a sudden load step request at constant engine speed. At the same time, simulation of transient turbocharger performance is rather challenging, because the initial spinning speed is low, while the turbine is fully loaded. This is a difficult-to-capture combination for conventional mapping techniques and substantial extrapolation must be applied. Comparison of fitting methods with the gas stand map is provided in Figure 23.

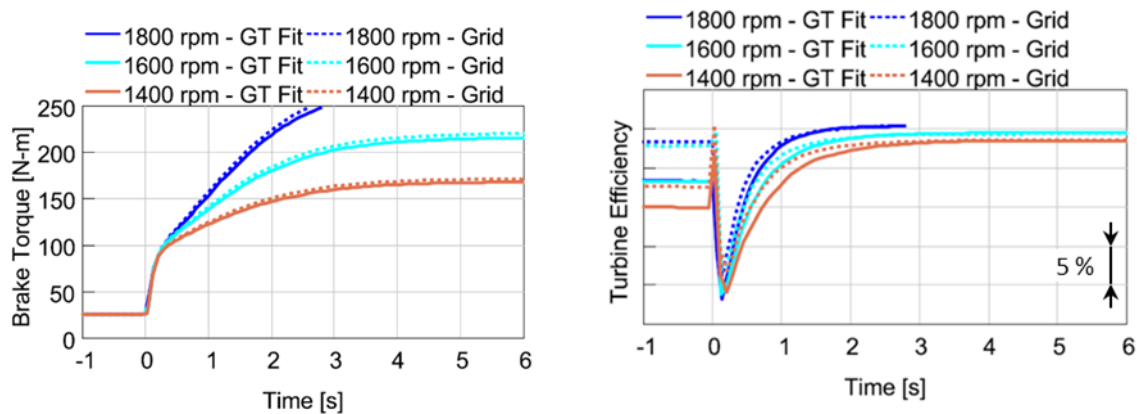


Figure 23: Engine brake torque (left) and cycle-average turbine efficiency (right) at constant engine speeds with the gas stand map



Overall, the transient engine performance with the default and the proposed fitting of the gas stand map is very similar, which, together with the steady-state comparison, confirms a good agreement between both methods (see Figures 21 & 23). Despite that, a small advantage can be identified with the proposed fitting algorithm.

In the case of the dyno map, however, a much bigger difference can be recognized between the speeds of increase of the brake torque. The reason is the significantly lower cycle-average turbine efficiency (isentropic power weighted) at the beginning of each load step with the default turbine fitting method (see Figure 24).

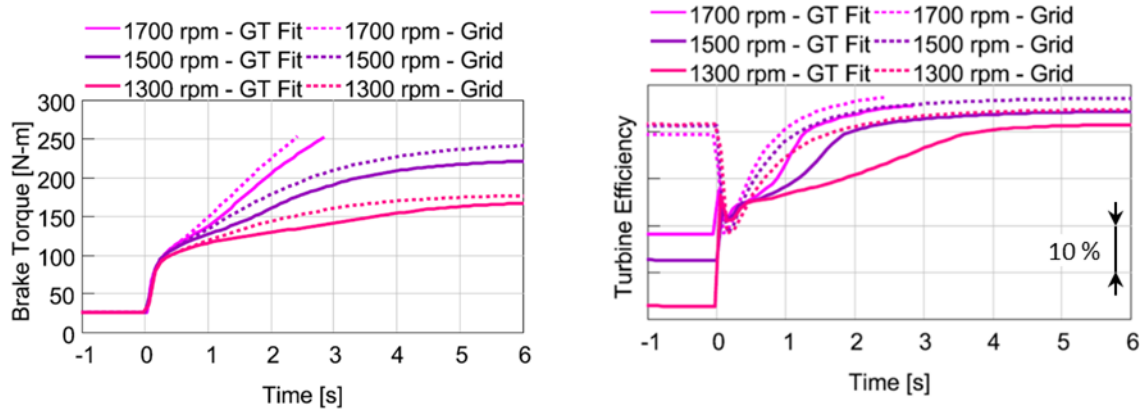


Figure 24: Engine brake torque (left) and cycle-average turbine efficiency (right) at constant engine speeds with the dyno map

Fully extrapolated dyno maps are overlaid in Figure 25 for comparison. It is obvious that the default fitting method predicts much lower maximum efficiency at low corrected speeds, which are relevant in the beginning of engine load steps. The advantage of the proposed algorithm is that it predicts the maximum efficiency with the help of minimization of fit error at sub-optimal operating points. On the contrary, the highest measured efficiency is not exceeded with the default one.

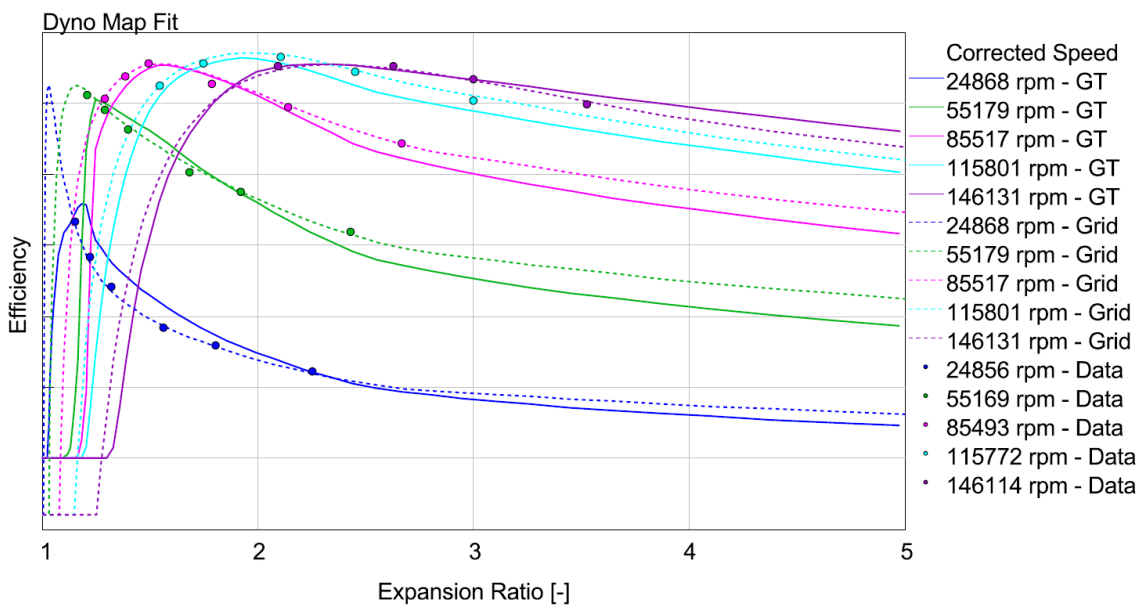


Figure 25: Extrapolated dyno map fitted by the default and the proposed methods



## CONCLUSION

At the beginning of this dissertation project was the need for a tool that would facilitate postprocessing of measured turbine maps of automotive turbochargers. This involves performance data management in the first place, but also its visualisation and numerical treatment to enable back-to-back comparisons. Furthermore, to assess the differences at equal operating conditions, efficiency and corrected mass flow rate must be interpolated or extrapolated depending on the distribution of measured operating points. Therefore, the input data must first be fitted by a convenient turbine model.

The implementation of a turbine fitting algorithm is the main objective of this work. For that purpose, a MATLAB<sup>TM</sup> application has been developed, which enabled testing of different numerical procedures. The first step was to understand the existing industrial practice and use it to establish the baseline method. The algorithm included in GT-SUITE<sup>TM</sup> was chosen, because it represents a state-of-the-art solution that is widely used in the industry. However, the process is not exhaustively documented in available information sources, so custom procedures had to be proposed where necessary (see [10, 20]). Therefore, the baseline turbine fitting method, as implemented in the MATLAB application, is not fully representative of the one integrated in GT-SUITE. Nevertheless, it was possible to conclude that the declared linear relationship between the optimum blade speed ratio and the expansion ratio does not allow the proper extrapolation of the corrected mass flow rate. This was the main motivation for the development of a custom process.

The main difference between the proposed and baseline turbine models is that the new model features the *choke phenomenon*. Consequently, optimum blade speed ratio is limited above the critical expansion ratio in such a way that optimum corrected speed remains constant. Also, emphasis is placed on the implementation of physics principles to improve the fidelity of extrapolation. The theory of *radial equilibrium* is used to quantify the effect of centrifugal force on the corrected mass flow rate at low expansion ratios. Further, by the new structure of characteristic functions, it is ensured that corrected mass flow rate at each speed line is non-decreasing with expansion ratio. That is the expected behaviour based on an analogy with the discharge through an *ideal nozzle*.

Thanks to the application of *optimization methods* to identify the properties of turbine performance models, it is possible to estimate the maximum efficiency in situations, where this maximum is not included among input data points. The mechanism is based on the assumption that minimization of fit error at sub-optimal operating points can be used to determine the maximum efficiency at the same expansion ratio. Repetitive refinement of this relationship during the complete fitting process ensures reasonable results without impacting convergence.

Initial testing confirmed that the method is functional and robust when fitting the outputs of hot gas stand and turbine dynamometer measurements. With the help of a higher-level approximation, it is possible to visualize performance trends related to the variability of the A/R parameter. A similar approach is followed to plot the

relationship between maximum efficiency and optimum corrected mass flow rate across multiple turbine sizes. As the last step, exported turbine performance models are used within engine steady state and transient load step simulations in GT-SUITE (in the so-called *grid* format). In the case of the sample gas stand map, both algorithms (GT-SUITE default and the proposed one) result in similar engine performance at steady state and transients. However, with the default fit of the dyno map, transient engine performance is compromised by overly conservative efficiency extrapolation to low corrected turbine speeds.

The further evolution of the proposed turbine fitting procedure will involve mainly a refinement of the middle part of the optimum blade speed ratio spline (the section between the transition and the choke points in Figure 15). As per the current definition, the end-slopes are controlled, but the curvature is not. Besides, the MATLAB application will be extended with additional post-processing features. As of now, variable nozzle geometry, twin-scroll and sector-divided technologies are not supported, but the proposed methodology is well suited for this extension. A strong new trend calls for a separate treatment of the different aspects of turbocharger modelling. Namely, the heat transfer and bearing friction, both of which are normally included in compressor and turbine maps obtained by hot gas stand measurements. It will be advantageous to remove and model these effects independently to use gas stand maps in simulations.

## REFERENCES

- [1] HEYWOOD, J. B. *Internal Combustion Engine Fundamentals*. 1<sup>st</sup> ed. New York: McGraw-Hill, 1988. ISBN 007028637X.
- [2] WATSON, N., JANOTA, M. S. *Turbocharging the Internal Combustion Engine*. 1<sup>st</sup> ed. London: The Macmillan Press Ltd., 1982. ISBN 0333242904.
- [3] BAINES, N. *Fundamentals of Turbocharging*. 1<sup>st</sup> ed. Vermont: Concepts NREC, 2005. ISBN 0933283148.
- [4] KADRNOŽKA, J. *Lopatkové stroje*. 1<sup>st</sup> ed., edited. Brno: Akademické nakladatelství CERM, 2003. ISBN 80-720-4297-1.
- [5] HIERETH, H. and PRENNINGER, P. *Charging the internal combustion engine*. 1<sup>st</sup> ed. Wien: Springer-Verlag, 2007. ISBN 9783211330333.
- [6] KLAPKA, J. *Metody operačního výzkumu*. 2<sup>nd</sup> ed. Brno: VUTIUM, 2001. ISBN 80-214-1839-7.
- [7] ČERMÁK, L. and HLAVIČKA, R. *Numerické metody*. 2<sup>nd</sup> ed. Brno: Akademické nakladatelství CERM, 2008. ISBN 978-80-214-3752-4.
- [8] KARPÍŠEK, Z. *Matematika IV: statistika a pravděpodobnost*. 3<sup>rd</sup> ed., appended. Brno: Akademické nakladatelství CERM, 2007. ISBN 978-80-214-3380-9.
- [9] PAVELEK, M. *Termomechanika*. Brno: Akademické nakladatelství CERM, 2011. ISBN 978-80-214-4300-6.
- [10] PESYRIDIS, A., SALIM, W. S-I. W. and MARTINEZ-BOTAS, R. F. Turbocharger Matching Methodology for Improved Exhaust Energy Recovery. In *Institution of Mechanical Engineers: 10th International Conference on Turbochargers and Turbocharging, 15-16 May, 2012*. Cambridge: Woodhead Publishing Ltd., 2012. p. 203-218. ISBN 9780857096135.
- [11] THEOTOKATOS, G. and KYRTATOS, N. P. Diesel Engine Transient Operation with Turbocharger Compressor Surging. *SAE Technical Paper 2001-01-1241*, 2001, ISSN 0148-7191, DOI 10.4271/2001-01-1241.
- [12] SHAABAN, S. and SEUME, J. Impact of Turbocharger Non-Adiabatic Operation on Engine Volumetric Efficiency and Turbo Lag. *International Journal of Rotating Machinery*, 2012, vol. 2012, Article ID 625453, DOI 10.1155/2012-625453.
- [13] CERDOUN, M. and GHENAIET, A. Unsteady behaviour of a twin entry radial turbine under engine like inlet flow conditions. *Applied Thermal Engineering*, 2018, vol. 130, p. 93-111. ISSN 1359-4311, DOI 10.1016/j.applthermaleng.2017.11.001.
- [14] LÜDDECKE, B., FILSINGER, D. and BARGENDE, M. On Wide Mapping of a Mixed Flow Turbine with Regard to Compressor Heat Flows during Turbocharger Testing. In *Institution of Mechanical Engineers: 10th*

*International Conference on Turbochargers and Turbocharging, 15-16 May, 2012. Cambridge: Woodhead Publishing Ltd., 2012, p. 185-202. ISBN 9780857096135.*

- [15] BOZZA, F. and DE BELLIS, V. Steady Modeling of a Turbocharger Turbine for Automotive Engines. *ASME Journal of Engineering for Gas Turbines and Power*, 2014, vol. 136, issue 1. ISSN 0742-4795, DOI 10.1115/1.4025263.
- [16] DE BELLIS, V., BOZZA, F., SCHERNUS, C. and UHLMANN, T., Advanced Numerical and Experimental Techniques for the Extension of a Turbine Mapping. *SAE International Journal of Engines*, 2013, vol. 122, issue 3, p. 1771-1785. ISSN 1946-3936, DOI 10.4271/2013-24-0119.
- [17] JENSEN, J.-P., KRISTENSEN, A. F., SORENSON, S. C., HOUBAK, N. and HENDRICKS, E. Mean Value Modeling of a Small Turbocharged Diesel Engine. *SAE Technical Paper No. 910070*, 1991, ISSN 0148-7191, DOI 10.4271/910070.
- [18] SHEN, Y., LI, C., HEIMONEN, A., MEURMAN, J. H., NUNN, M. E., MILLER, D. R., VAN DYKE, T. E., BOLLU, P., KAAJA, R. and JANKET, S. A pilot study on maternal oral health and birth weight of twins. *Open Journal of Epidemiology*, 2014, vol. 4, p. 7-13. DOI 10.4236/ojepi.2014.41002.
- [19] SIRAKOV, B., CASEY, M. V. Evaluation of Heat Transfer Effects on Turbocharger Performance. In *Proceedings of the ASME 2011 Turbo Expo: Turbine Technical Conference and Exposition. Volume 7: Turbomachinery, Parts A, B, and C*. Vancouver, British Columbia, Canada. June 6–10, 2011. pp. 2075-2086. ASME. DOI 10.1115/GT2011-45887
- [20] GAMMA TECHNOLOGIES. *GT-SUITE: GT-SUITE Flow Theory Manual*. GT-SUITE v.2016, Gamma Technologies, LLC., Westmont, IL., US
- [21] AUSTRALIAN TURBO. *Turbocharger cutaway* [online]. 2014 [cited 2014-12-28]. Available on: <http://australianturbo.com.au/images/Blog/Blog%20Pictures/Cutaway.jpg>
- [22] WIKIPEDIA. *Flat spline* [online]. 2020 [cited 2020-11-17]. Available on: [https://commons.wikimedia.org/wiki/File:Spline\\_\(PSF\).png](https://commons.wikimedia.org/wiki/File:Spline_(PSF).png)
- [23] GAMMA TECHNOLOGIES. *GT-SUITE* [online]. 2020 [cited 2020-8-2]. Available on: <https://www.gtisoft.com>
- [24] MATHWORKS. *MATLAB* [online]. 2020 [cited 2020-8-23]. Available on: <https://www.mathworks.com>
- [25] MATHWORKS. *MATLAB SQLite 3 driver* [online]. 2019 [cited 2019-10-21]. Available on: [https://uk.mathworks.com/matlabcentral/fileexchange/57123-kyamagu-matlab-sqlite3-driver?s\\_tid=srchtitle](https://uk.mathworks.com/matlabcentral/fileexchange/57123-kyamagu-matlab-sqlite3-driver?s_tid=srchtitle)
- [26] CONCEPTS NREC. *RITAL* [online]. 2021 [cited 2021-6-27]. Available on: <https://www.conceptsnrec.com/solutions/software/computer-aided-engineering/preliminary-design/rital>

## AUTHOR'S CV

Name: Adam Vondrák  
Date of birth: 10<sup>th</sup> January 1990  
Permanent address: Zatloukalova 67, 62100 Brno, Czech Republic

### **Educational background:**

- 2015-2021 Design and Process Engineering, Faculty of Mechanical Engineering, Brno University of Technology, Ph.D. programme
- 2013-2014 Automotive Engineering, Faculty of Engineering Design, Production Engineering and Automotive Engineering, University of Stuttgart, Erasmus Programme
- 2012-2015 Automotive Engineering, Faculty of Mechanical Engineering, Brno University of Technology, master's programme
- 2009-2012 Mechanical Engineering, Faculty of Mechanical Engineering, Brno University of Technology, bachelor's programme
- 2001-2009 Grammar School Brno-Řečkovice

### **Teaching activities within the Ph.D. study:**

- Supervision of bachelor and master theses
- Host lectures on the modelling of multi-physical systems in GT-SUITE as part of the subject Theory of Combustion Engines (QTS)
- Student workshops (turbocharging of a Formula Student engine for TU Brno Racing, introduction to the technology of turbochargers for selected students at Garrett Motion and as part of Techfest 2016 & 2017)

### **Professional experience:**

- since 2018 Systems Engineer, Garrett Motion Czech Republic s.r.o.
- 2015-2018 Systems Engineer, Honeywell, spol. s r.o. - HTS CZ o.z.
- 2014-2015 Student Application Engineer, Honeywell, spol. s r.o. - HTS CZ o.z.

### **Other skills:**

- Languages Czech (native), English (C1, CAE certificate), German (B2)
- Software GT-SUITE (professional), MATLAB (advanced), MS-Office (regular user), PTC Creo (intermediate), CATIA (intermediate), ANSYS CFX (beginner)
- Licenses Driver's license (B, C, D, E)

## **ABSTRACT**

Modelling of turbine performance is a prerequisite for detailed simulation of gas exchange in turbocharged combustion engines. At the same time, the possibility to determine efficiency and mass flow capacity at arbitrary operating points is key to comparing different turbine stages. The objective of this work is to propose a single method for both purposes, so it is possible to do the comparison using exactly the same turbine performance model as in subsequent engine working cycle simulation. The source of input data is typically a gas stand measurement, which enables capturing of limited turbine operating range only. In this work, methods are proposed to improve the fidelity and robustness of turbine performance extrapolation, while optimization is employed to find the best fit in terms of agreement between the model and the input data.

## **ABSTRAKT**

Modelování turbínových charakteristik je nutným předpokladem pro detailní simulaci výměny náplně válce turbodmychadlem přeplňovaných spalovacích motorů. Kromě toho je možnost stanovení účinnosti a průtokové kapacity v libovolných pracovních bodech klíčová pro porovnání různých turbínových stupňů. Cílem této práce je předložit jednotnou metodu pro oba účely tak, aby bylo možné provést porovnání použitím přesně stejných modelů turbín jako při následné simulaci pracovního oběhu motoru. Zdrojem vstupních dat je obvykle měření na plynové zkušebně, které však umožňuje zachycení pouze omezeného pracovního rozsahu turbíny. V této práci jsou navrženy metody umožňující zvýšení věrohodnosti a robustnosti extrapolace turbínových charakteristik, přičemž optimalizace je využita k určení takových parametrů hledaných funkcí, které vedou k nejlepší shodě mezi modelem a vstupními daty.